Medical Engineering and Physics 68 (2019) 57–64

Contents lists available at ScienceDirect

Medical Engineering and Physics

journal homepage: www.elsevier.com/locate/medengphy

# Gap between the fragment and the tibia affects the stability of tibial tubercle osteotomy: A finite element study

Yen-Nien Chen[a,b,1], Chih-Wei Chang[b,c,d,1], Chih-Han Chang[b], Chi-Rung Chung[e,*], Chun-Ting Li[f,**], Yao-Te Peng[b,g]

[a] Department of Orthopedics, Show Chwan Memorial Hospital, Changhua, Taiwan
[b] Department of BioMedical Engineering, National Cheng Kung University, Tainan, Taiwan
[c] Department of Orthopedics, College of Medicine, National Cheng Kung University, Tainan, Taiwan
[d] Department of Orthopedics & Joint Reconstruction Center, National Cheng Kung University Hospital, College of Medicine, National Cheng Kung University, Tainan, Taiwan
[e] Department of Orthopedics, Chi-Mei Medical Center, Tainan, Taiwan
[f] Graduate Institute of Mechatronic System Engineering, National University of Tainan, Tainan, Taiwan
[g] Metal Industries Research & Development Centre, Kaohsiung, Taiwan

A R T I C L E I N F O

*Article history:*
Received 8 March 2018
Revised 2 March 2019
Accepted 30 March 2019

*Keywords:*
Tibial tubercle osteotomy
Gap
Fragment location
Screw configuration
Finite element method

A B S T R A C T

Tibial tubercle osteotomy (TTO) is commonly performed in cases of complicated juxta-articular trauma or revision total knee arthroplasty. However, strategies for firmly fixing the resulting osteotomy bone fragment are not sufficiently understood. This study aims to investigate the effect of the location of the gap between the fragment and the tibia and with various fixed screw configurations on TTO stability, contact force on the fragment, and bone stress by using the finite element method. A TTO model with a 1-mm gap, either above or below the fragment, was developed. Furthermore, five screw configurations, including two parallel horizontal screws placed at 20- and 30-mm intervals, two parallel downward screws, two trapezoid screws, and two divergent screws, were used. A vertically upward 1600-N force was applied on the tibial tubercle to mimic a worst-case condition. Placing the fragment close to the superior cutting plane (above the gap) yielded greater stability and less stress on the bone than did placing it close to the inferior cutting plane. The superior cutting plane of the tibia generated the largest contact force on the superior plane of the fragment for static balance under loading. Additionally, among all screw configurations, the configuration involving two parallel downward screws resulted in the highest stability but also the greatest stress on the cortical bone. The fragment obtains a solid barrier and support from the tibia immediately after surgery to against the patellar tension force when the fragment is close to the superior cutting plane of the tibia.



## 1. Introduction

Tibial tubercle osteotomy (TTO) is commonly performed to expand the surgical exposure and field, create negligible soft tissue violation, and protect the patellar tendon in cases of complicated juxta-articular trauma or revision total knee arthroplasty (RTKR) [1–11]. The strengths of TTO are its predictable recovery through bone healing and its feasible outcomes [12–16]. However, a relatively high rate of complications, such as nonunion, fracture, tubercle fragment displacement, and tibial metaphyseal fracture, has been reported [10]. Most complications following TTO are generally related to the fixation of the osteotomy. Nevertheless, there is little understanding of how to firmly fix the osteotomy tubercle fragment back to the tibia after osteotomy. A few academic studies have been conducted to investigate mechanical stability; however, the internal mechanical responses, including the stress and contact force on the TTO bone fragment, are still unclear.

Previous research has suggested that TTO fixation may be achieved by means of a step cut above the insertion site of the patellar tendon at the proximal tibia and screw fixation has been suggested for TTO fixation [9,10,16–18]. In clinical practice,

* Corresponding author at: Department of Orthopedics, Chi-Mei Medical Center, Tainan, Taiwan.
** Corresponding author at: Graduate Institute of Mechatronic System Engineering, National University of Tainan, Tainan, Taiwan.
*E-mail addresses:* yennien.chen@gmail.com (Y.-N. Chen), u7901064@yahoo.com.tw (C.-W. Chang), changbmencku@gmail.com (C.-H. Chang), dinosaur5695@hotmail.com (C.-R. Chung), ctli0412@gmail.com (C.-T. Li), yautepeng@gmail.com (Y.-T. Peng).
[1] Both authors contributed equally to this work.

https://doi.org/10.1016/j.medengphy.2019.03.012

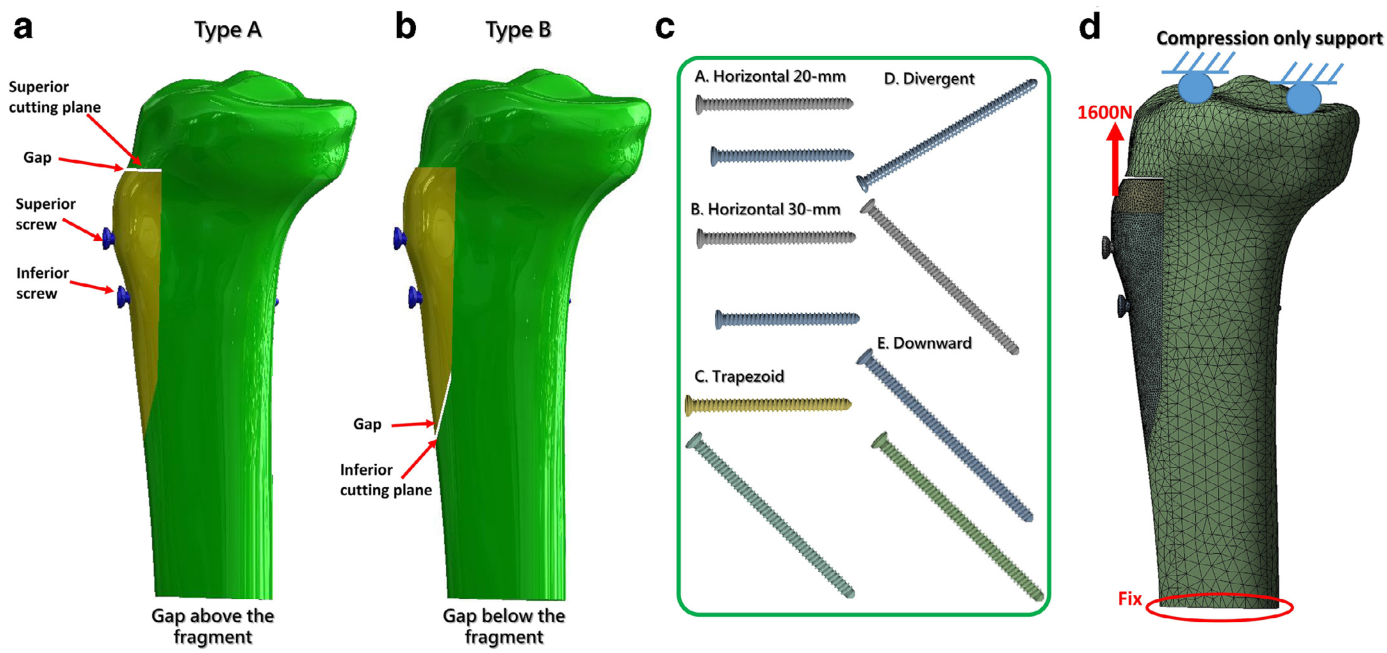


**Fig. 1.** TTO models (a) and (b), screw configurations (c) and boundary condition (d) used in this study.

however, the cut bone fragment is slightly shorter than the slot of the tibia because of the thickness of the saw, which causes a gap between the osteotomized bone fragment and the tibia when the bone fragment is fixed back to the tibia. How to deal with the gap, either by placing the fragment close to the superior cutting plane and above the gap or by placing the fragment close to the inferior cutting plane and below the gap, has not been mentioned in the literature. Moreover, only configurations involving two parallel horizontal screws have been used in mechanical studies [17,18] and the other screw configurations, such as trapezoid and parallel downward, have not been employed. The surgeon must adjust the trajectory of the screw due to poor bone condition or to avoid the artificial joint component in revision surgery, but no mechanical study has reported on stability with various screw configurations. From a mechanical perspective, the screw configuration and fragment–tibia gap are critical for the stability of the TTO bone fragment. Enabling contact between the fragment and the tibial bone when loading is applied on the fragment can share the loading on the fragment with the tibial bone, thereby increasing the stability of the fragment.

In addition to stability, the internal mechanical status, including the stress and contact forces on the bone fragment after static balance, remains unknown. Furthermore, complications due to fractures of bone fragments—particularly near the junction of the bone and metallic screws—are a primary concern in clinical applications [12,19–21]. The stress on the bone, particularly near the screw holes, is critical to the bone fragment because high stress is a potential factor causing bone failure. However, bone stress is difficult to detect because no sensor is sufficiently small to be placed into a sample without disturbance. By contrast, the finite element (FE) method is a numerical method for calculating the internal stress and strain of a model without destroying the model [22–24]. Therefore, the aim of this study was to investigate the effect of the location of the gap between the fragment and the tibia and with various fixed screw configurations on TTO stability, internal contact force on the fragment, and bone stress by using the FE method. Stability was evaluated by fragment displacement and the deformation of the gap between the fragment and the tibia.

## 2. Methods

To investigate the effect of the location of the fragment and the location of the gap between the fragment and the tibia on the biomechanical responses of TTO with various screw configurations, an FE model was developed; the model comprised a tibia with TTO fixed with various screw configurations. The stability of TTO was evaluated by examining the displacement of the fragment and the deformation of the gap between the fragment and the tibia. Moreover, the maximum principal stress of the bone and the contact forces on the fragment were demonstrated.

### 2.1. Solid model

An intact solid tibia model was created based on computed tomography (CT) images provided by the US National Institutes of Health in its Visible Human Project. The images were taken with 1-mm intervals, and the contours of the cortical bone were retrieved according to their gray values by using Avizo Version 6 software (VSG SAS, Bordeaux, France). The cancellous bone was created by shrinking 2 mm of the cortical bone [25] because of the blurry boundary between the cortical and cancellous bone at the proximal tibia. The solid bone model was then imported into the CAD software SolidWorks 2012 (Dassault Systemes SolidWorks Corp., Waltham, MA, USA) to create the osteotomy and implant screws. The tibial tubercle was isolated from the tibia, and a 1-mm-thick bone sheet was resected from the top of the fragment to simulate bone loss from a saw blade. The bone fragment was 85 mm long and 15 mm thick [9,10,14,17,18]. The bone fragment was kept at the original position with a 1-mm gap above the fragment between the fragment and the tibia (type A; Fig. 1(a)) or moved upward close to the superior cutting plane with a gap below the fragment (type B; Fig. 1(b)). The cut fragment was fixed to the tibia with two cortical screws (outer diameter, 4.5 mm; Synthes, PA, USA). The length of the horizontal screws was 54 mm (VA401.054), whereas that of the other screws was 76 mm (VA401.076). Two intervals, namely 20 and 30 mm, were considered between the two parallel horizontal screws [17], whereas the interval between the two parallel downward screws was 15 mm. The angles between the two

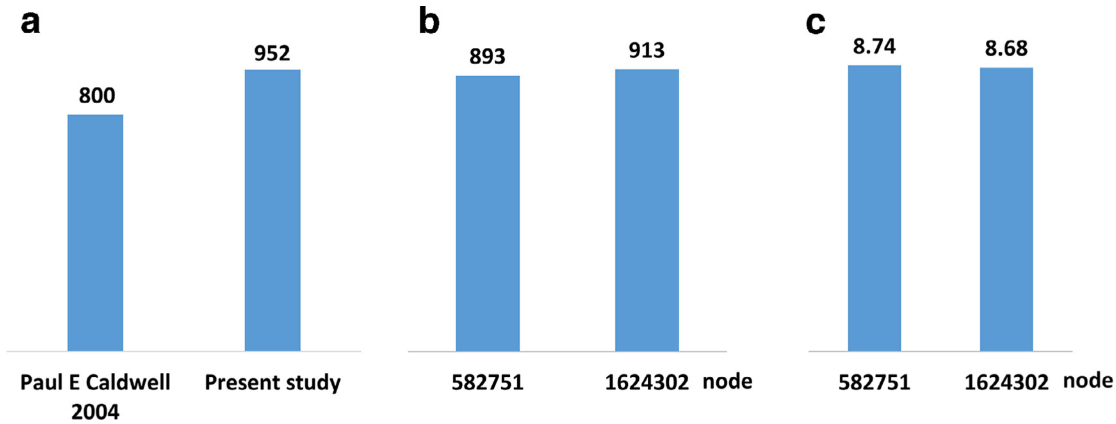


**Fig. 2.** Comparison of the tubercle stiffness (N/mm) in the present study with that of Paul (a). Comparison of the contact force (N) on the superior cutting plane of the bone fragment (b) and the maximum principle stress (MPa) of the tibia near the screw hole (c) in 582,751 and 1,624,302 nodes.

screws were 45° and 90° in the trapezoid and divergent configurations, respectively. In total, five feasible types of screw configurations were used in the simulation, including two parallel horizontal screws with intervals of 20 and 30 mm, two parallel downward screws, two trapezoid screws, and two divergent screws (Fig. 1(c)).

### 2.2. FE model

The constructed solid models were imported into ANSYS WORKBENCH V17 (Swanson Analysis, Houston, PA, USA) to mesh and achieve the simulation. A quadratic element (solid 187) was used to mesh all model parts. The mesh density of the screws, bone fragment, and thread areas in the tibia was increased by local refinement in ANSYS WORKBENCH V17. In total, 556,572 nodes and 380,715 elements were used in the model with the horizontal screw configuration. Each FE model with various screw configurations was meshed with uniform mesh settings. The contact behaviors between the cutting planes of the tubercle fragment and the cutting planes of the tibia and between the thread surfaces of the screws and the surrounding bone were defined for frictional surface-to-surface contact (contact 174 and target 170, ANSYS). The frictional coefficients of bone-to-bone and bone-to-metal (screw) contact were set to 0.45 and 0.3, respectively [24].

### 2.3. Material property and boundary condition

The elastic modulus values of the cortical and cancellous bones were set to 12.6 GPa and 457 MPa [26,27], respectively, and the Poisson ratios were both set to 0.3. Because the screw used in the present study was titanium, the elastic modulus and Poisson ratios were set to 110 GPa and 0.3, respectively [28]. A vertically upward 1600-N force, divided into 12 equal forces on 12 points, based on an experimental study was applied on the tibial tubercle at the insertion site of the patellar tendon to simulate the pulling force from the quadriceps muscle [17,18]. The purpose of this application was to mimic a worst-case condition in which the tubercle sustained a high tension force from the patellar tendon, such as the force sustained from initially standing or stepping up, when the bilateral end of the tibia was constrained by the ankle and knee joint. The magnitude of the force was defined based on the failure load in the cadaveric TTO tibia. The entire superior surface of the tibia was set to compression-only support, which meant the surface could bear only normal force instead of tension force, to simulate resistance from the distal femoral condyle. The distal surface of the tibia was totally fixed (Fig. 1(d)).

### 2.4. Validation and convergence

To confirm the reality of the present model, the results of the TTO model with two horizontal screws and without the compression-only support were compared with Caldwell's et al. study [18] for validation. The difference of tubercle stiffness between Caldwell's study and the present study was 16% (Fig. 2(a)). Furthermore, a mesh convergence test was conducted by globally increasing the numbers of nodes and elements. The differences, between the 582,751 and 1,624,302 nodes, in the contact force on the superior surface of the bone fragment and maximum principal stress near the screw hole of the tibia shift were 2.8% and 1.9%, respectively (Fig. 2(b) and (c)). Finally, the same element size setting with that used in the model comprising 582,751 nodes was used in the simulation.

## 3. Results

The type B fragment resulted in greater stability with less fragment displacement than the type A (Fig. 3). Among all screw configurations, the configuration involving two parallel downward screws resulted in the smallest bone fragment displacement, whereas the horizontal screw configuration resulted in the largest displacement. Furthermore, the type B fragment resulted in a smaller difference in fragment displacement between the screw configurations (0.236–0.333 mm), compared with the type A (0.375–0.977 mm). Additionally, the type B fragment resulted in a more stable structure with a smaller gap deformation between the fragment and the vertical and inferior cutting planes than the type A (Table 1). The configuration involving two parallel downward screws facilitated the smallest gap deformation. Among the other configurations, the trapezoid and divergent configurations facilitated a smaller gap deformation than did the configuration involving two parallel horizontal screws.

In the type B fragment, the superior cutting plane of the tibia generated the largest contact force on the fragment for static balance after a load was added. The peak contact force values were 1397 and 893 N in the two parallel horizontal and downward screw configurations, respectively (Table 2). Although the contact force on the fragment in the two downward configuration was smaller than that in the two horizontal configuration, the maximum difference in the contact force between the screw and superior cutting plane of the tibia was smaller in the downward (292–839 N) than in the horizontal (74–1397 N) configuration. The two parallel screw configurations (horizontal and downward) resulted in a smaller difference in screw contact force between the two

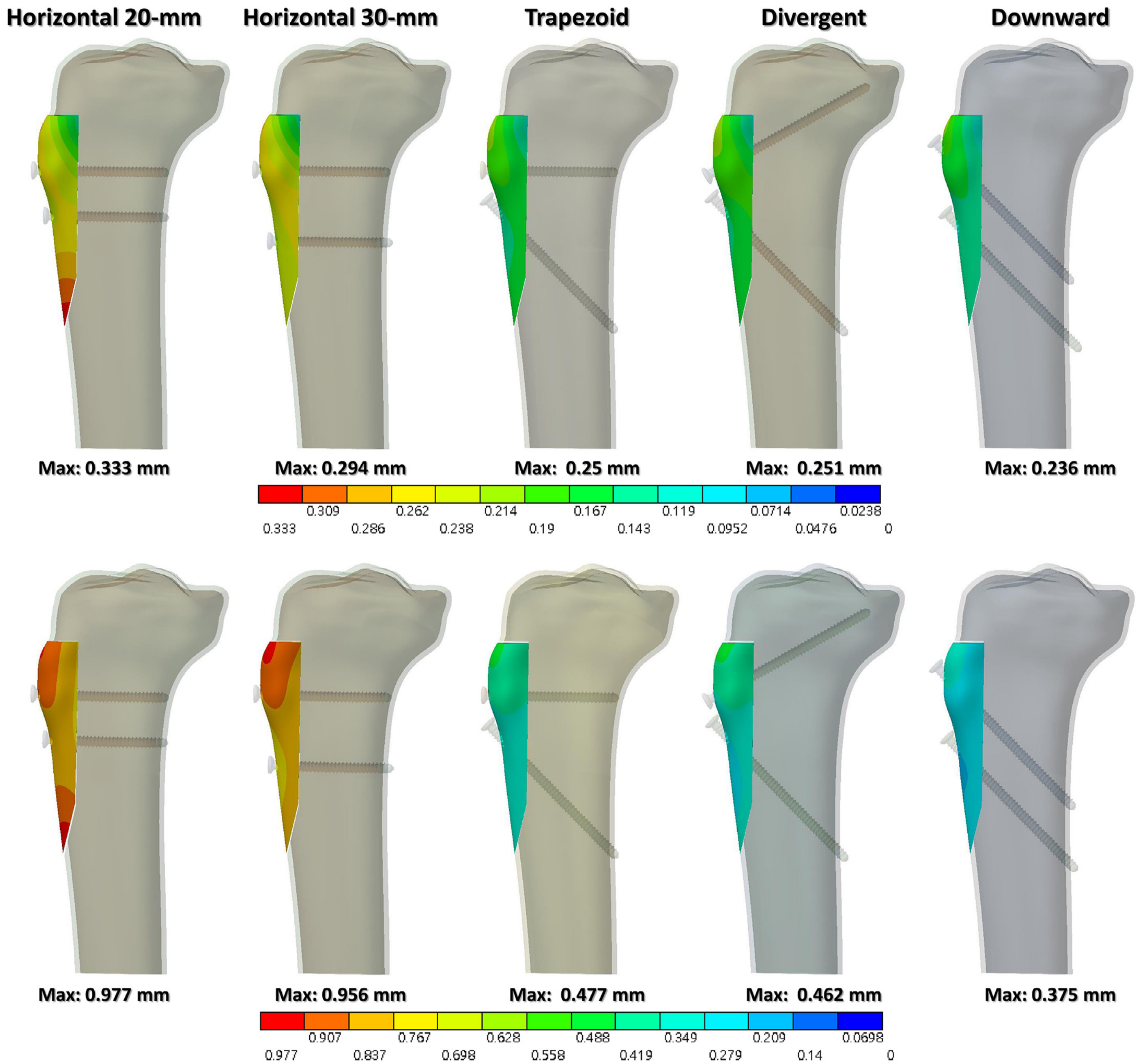


**Fig. 3.** Total displacement of the fragment close to the superior (top row; type B) and inferior (bottom row; type A) cutting planes of the tibia and with various screw configurations.

**Table 1**
Maximum gap deformation (mm) between the fragment and the tibia.

| | Horizontal D20 mm | Horizontal D30 mm | Trapezoid | Diverge | Downward |
|---|---|---|---|---|---|
| **Fragment close to the superior cutting plane and above the gap** | | | | | |
| Between superior cutting plane and fragment | 0 | 0 | 0 | 0 | 0 |
| Between vertical cutting plane and fragment | 0.16 | 0.11 | 0.04 | 0.06 | 0.03 |
| Between inferior cutting plane and fragment | 0.48 | 0.35 | 0.29 | 0.28 | 0.28 |
| **Fragment close to the inferior cutting plane and below the gap** | | | | | |
| Between superior cutting plane and fragment | 0.83 | 0.83 | 0.37 | 0.54 | 0.29 |
| Between vertical cutting plane and fragment | 0.48 | 0.22 | 0.03 | 0.07 | 0.02 |
| Between inferior cutting plane and fragment | 0.74 | 0.46 | 0.15 | 0.12 | 0.12 |

Two parallel horizontal screws with intervals of 20 (horizontal D20 mm) and 30 mm (horizontal D30 mm).

**Table 2**
Contact force (N) on the fragment.

| | Horizontal D20 mm | Horizontal D30 mm | Trapezoid | Diverge | Downward |
|---|---|---|---|---|---|
| **Fragment close to the superior cutting plane above the gap** | | | | | |
| Contact force on the superior cutting plane | 1397 | 1387 | 1008 | 1013 | 893 |
| Contact force on the vertical cutting plane | 22 | 19 | 37 | 17 | 45 |
| Contact force on the inferior cutting plane | 0 | 0 | 0 | 0 | 0 |
| Superior screw contact force | 74 | 80 | 60 | 57 | 292 |
| Inferior screw contact force | 126 | 132 | 510 | 526 | 382 |
| **Fragment close to the inferior cutting plane and below the gap** | | | | | |
| Contact force on the superior cutting plane | 0 | 0 | 0 | 0 | 0 |
| Contact force on the vertical cutting plane | 226 | 180 | 222 | 80 | 299 |
| Contact force on the inferior cutting plane | 0 | 0 | 0 | 0 | 0 |
| Superior screw contact force | 678 | 702 | 221 | 420 | 626 |
| Inferior screw contact force | 712 | 733 | 1164 | 1106 | 682 |

Two parallel horizontal screws with intervals of 20 (horizontal D20 mm) and 30 mm (horizontal D30 mm).

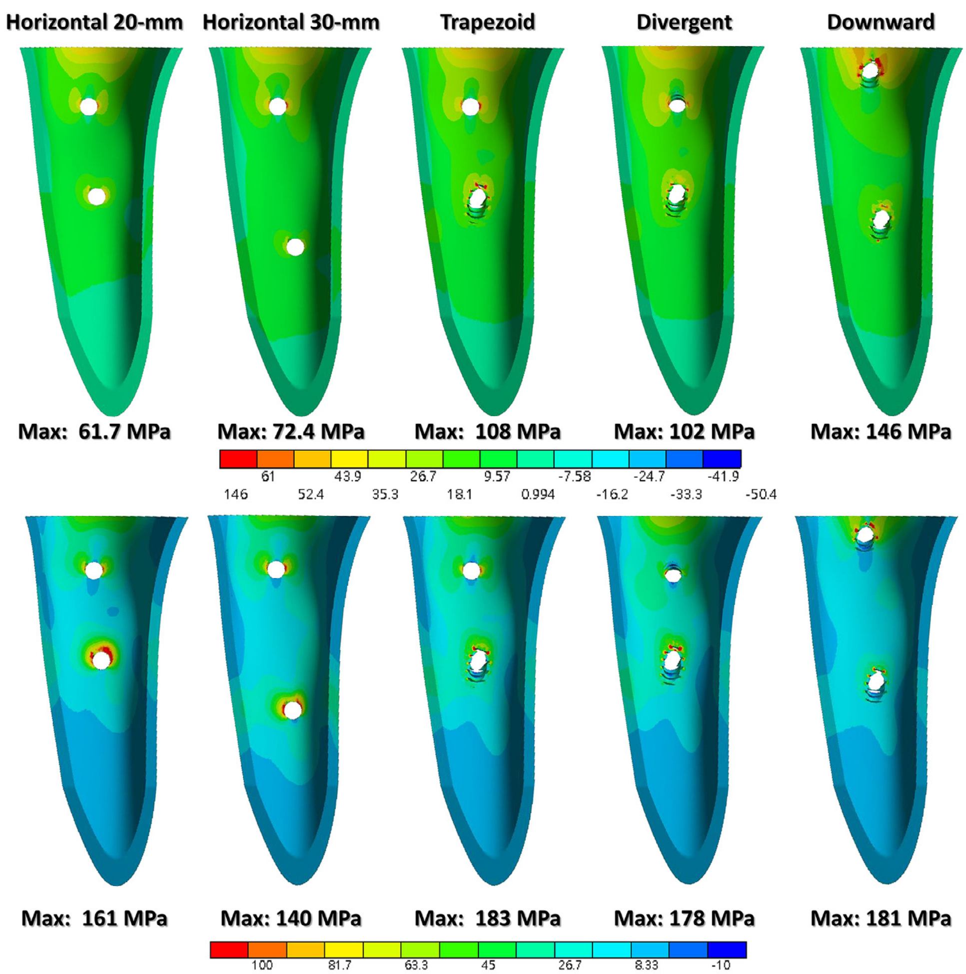


**Fig. 4.** Maximum principal stress in the cortical bone of the bone fragment close to the superior (top row; type B) and inferior (bottom row; type A) cutting planes of the tibia and with various screw configurations.

screws than did the two trapezoid and divergent configurations in an identical configuration. Although the contact force from the vertical cutting plane was increased with the type A fragment compared with the type B, the contact force remained much smaller than the screw contact forces.

Type B fragment resulted in a lower maximum principal stress in the tubercle fragment and the tibia than type A (Figs. 4–6). The maximum principal stress in the type A fragment increased up to 2.6 times (61.7–161 MPa, Fig. 4), 3.63 times (9.95–36.1 MPa, Fig. 5), and 4.79 times (8.02–38.4 MPa, Fig. 6) in the fragment cortex, fragment cancellous, and tibia, respectively, compared with the type B fragment in the horizontal screw configuration with an interval of 20 mm.

## 4. Discussion

TTO has become an increasingly popular procedure, particularly during RTKR, and its rising frequency is mirrored by the number of total knee arthroplasties performed currently. In this study, various managements of the gap between the fragment and the tibia in

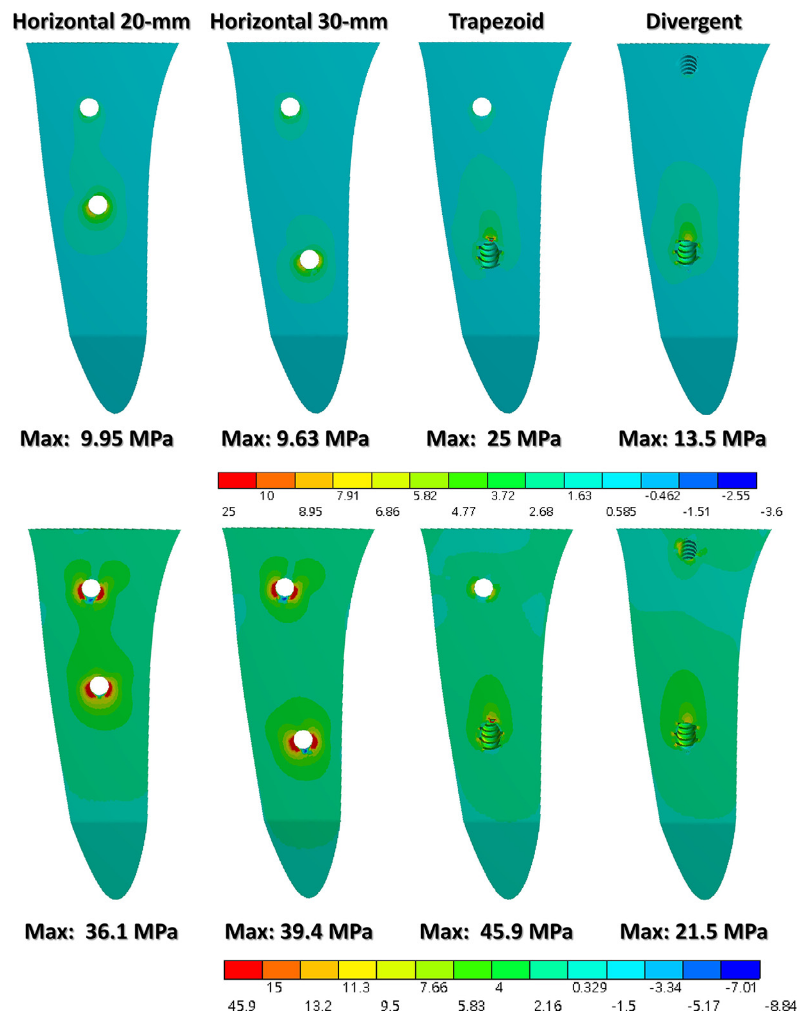


**Fig. 5.** Maximum principal stress in the cancellous bone of the bone fragment close to the superior (top row; type B) and inferior (bottom row; type A) cutting planes of the tibia and with various screw configurations.

TTO during the surgical procedure and the corresponding mechanical responses, including stability, internal stress, and force distribution of the tibia with various screw configurations, were demonstrated by FE models. The present results indicate that placing the fragment close to the superior cutting plane and above the gap (the type B fragment) increased TTO stability and decreased the stress in the bone and loading on the screws. By contrast, placing the fragment close to the inferior cutting plane and below the gap (the type A fragment) obviously decreased TTO stability and increased the stress in the bone and loading on the screws. Among all screw configurations, the configuration involving two parallel downward screws resulted in the highest stability with the least fragment displacement, in addition to leading to the highest stress in the bone fragment in the identical fragment location. The results provide a mechanical reference for surgeons to make a decision when applying the TTO technique in cases with complex and difficult situations in clinical practice.

The location of the gap between the fragment and the tibia affects TTO stability. In the type B fragment, no space exists between the superior cutting plane (loading site) of the tibia and fragment. The fragment obtains a solid barrier from the tibia with support immediately under a patellar tension force. The solid barrier prevents the fragment from moving upward and facilitates less displacement of the fragment, therefore resulting in less gap deformation between the vertical and inferior cutting planes of the tibia and fragment. By contrast, a 1-mm-wide space could exist between the fragment and the tibia before loading in the type A fragment. The screws must stop the fragment from migrating when the load begins to increase and they undertake almost all the load on the fragment. Although the vertical cutting plane provides the frictional force for the stability of the fragment, its contribution is much smaller than that of the screws.

Among the screw configurations, the configuration involving two parallel downward screws resulted in the most stable TTO structure. The maximum difference in fragment displacement between the screw configurations decreased in the type B fragment compared with the type A; this is because the loading on the fragment was distributed on the superior cutting plane and screws when the fragment was close to this plane. By contrast, the screws shouldered almost all the load when the fragment was close to the inferior cutting plane. Therefore, the effect of screw configuration on stability increases with the loading increased on the screws.

In clinical practice, the type B fragment is suggested because the force on the tubercle is shared by the superior cutting plane of the tibia and the two screws and it bypasses the tibia through the screws and bone instead of just the screws in the type A fragment. Furthermore, the contact force among bones, the tubercle fragment, and the tibia is helpful for promoting bone healing [29,30]. Surgeons may also adjust the force magnitude on the superior cutting plane with various screw configurations. In addition, the

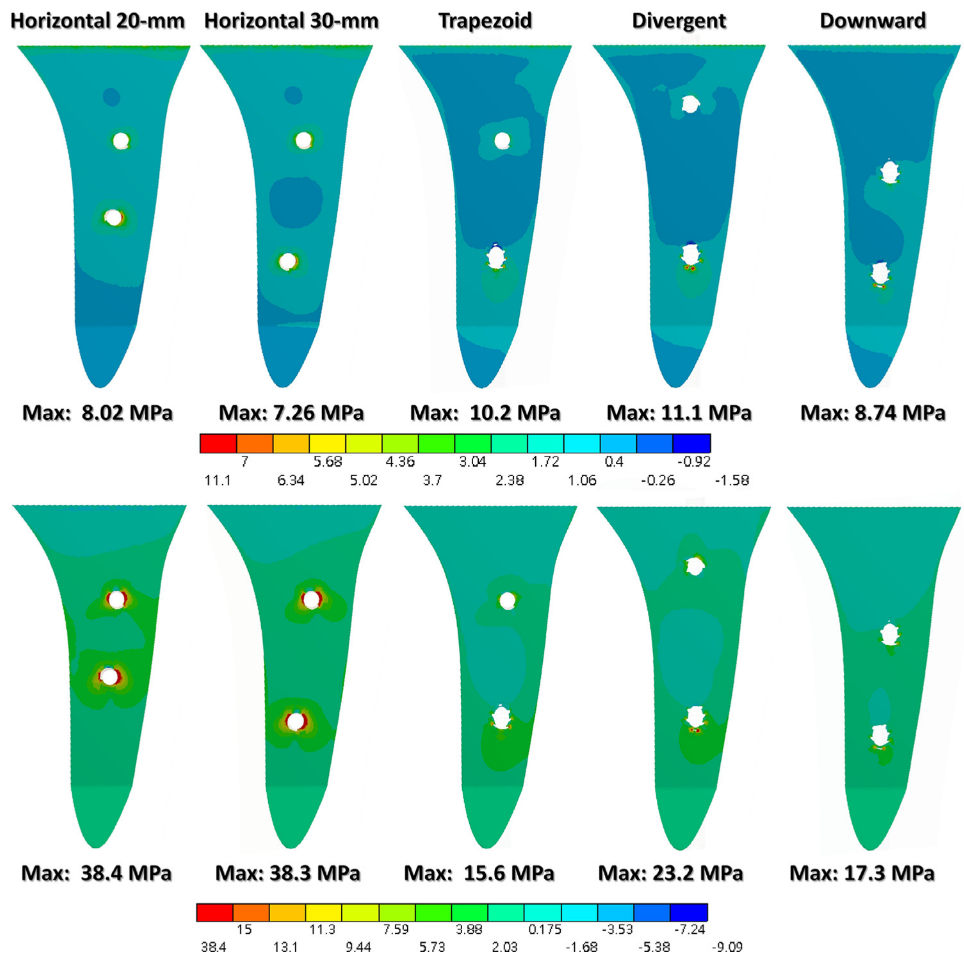


**Fig. 6.** Maximum principal stress in the cancellous bone of the vertical cutting plane of the tibia with fragment close to the superior (top row; type B) and inferior (bottom row; type A) cutting planes of the tibia and with various screw configurations.

type B fragment was observed to lead to lower stress in the bone fragment near the screw holes than the type A under identical screw configurations; this difference in stress is a result of the loading on the fragment being shared with the tibia bone through the superior cutting plane, thus decreasing the loading on the screws. Stress is a risk factor for bone failure, and low stress is recommended to avoid fragment rupture.

The configuration involving two parallel downward screws is an option, in addition to the current two parallel horizontal configuration, to increase TTO stability in cases involving severe bone loss and in situations in which the surgeon is unable to attach the fragment to the superior cutting plane of the tibia. Although the gap deformation and fragment displacement in the current configuration involving two parallel horizontal screws were larger than those in the trapezoid and divergent screw configurations, the difference in the screw contact forces between the two screws was smaller in the two parallel configuration than in the trapezoid and divergent configurations. Hence, force concentrated on one screw is not recommended in clinical practice because it increases the risk of bone failure.

The present study has some limitations. First, this model is based on a single tibia from the data in the NIH visible human project. The variation between subjects is not considered in the present simulation. Second, to clearly confirm the effects of fragment location in TTO, the tibial component of knee prostheses while revision were excluded in this study. Third, the cortex shell at the proximal tibia was set to a uniform thickness in the present mode, which might override the stiffness of the proximal tibia. The cutting plane in the present model was completely smooth; in clinical practice, small irregularities are unavoidable. Fourth, only a 1600-N patellar tendon force was considered. That force from quadriceps contraction was the major force on the tibia tubercle. The other constraint forces from the other muscles and the surrounding soft tissue, such as the ligament and joint capsule, were neglected. Besides, the proximal surface of the tibia was set to compression-only support, instead of restricting from the distal femur condyle. Fifth, the material properties were set to homogeneous and liner elastic; the nonlinear effect was not considered.

## 5. Conclusion

According to the results of this study, contact between the osteotomized tubercle fragment and the superior cutting plane of the tibia is critical for increasing the stability of TTO fragments because it provides a major contact force to resist the applied load on the bone fragment. Therefore, in TTO fixation with screws, this study recommends firmly placing the osteotomized tubercle fragment close to the superior cutting plane of the tibia to transfer the applied loading to the tibia, thus achieving high stability and low stress of the bone. Additionally, the configuration involving two parallel downward screws is an option for increasing TTO stability for cases involving severe bone loss and situations in which the surgeon is unable to attach the fragment to the superior cutting plane of the tibia. However, it must be considered carefully based on the subject's bone quality because of the higher stress to the cortical bone.

## Competing financial interests

Each author certifies that he or she has no commercial associations (e.g., consultancies, stock ownership, equity interest, patent/licensing arrangements, etc.) that might pose a conflict of interest in connection with the submitted article.

## Ethical approval

Not required.

## Acknowledgments

Chih-Wei Chang and Yen-Nien Chen contributed equally to this work. The authors express their gratitude to the Chi-Mei Medical Center (Taiwan) for the support for this study (CMNCKU10613). The authors also acknowledge the United States National Library of Medicine (NLM) and the Visible Human Project for the image data used to create the numerical model in this study. This manuscript was edited by Wallace Academic Editing.

## References

[1] Khan H, Grob K, Milne LP, Kuster MS. Tibial tubercle osteotomy to improve exposure in complex knee fractures: a cadaveric study and case series. Injury 2016;47:2331–8.
[2] Chinzei N, Ishida K, Kuroda R, Matsumoto T, Kubo S, Iguchi T, et al. Tibial tubercle osteotomy with screw fixation for total knee arthroplasty. Orthopedics 2014;37:e367–73.
[3] Lorbach O, Anagnostakos K, Kohn D. Osteotomy for approaches to the knee joint. Tibial tubercle, lateral epicondyle of the femur and head of the fibula. Orthopade 2013;42:332–40.
[4] Hirschmann MT, Hoffmann M, Krause R, Jenabzadeh RA, Arnold MP, Friederich NF. Anterolateral approach with tibial tubercle osteotomy versus standard medial approach for primary total knee arthroplasty: does it matter? BMC Musculoskelet Disord 2010;11:167.
[5] Della Valle CJ, Berger RA, Rosenberg AG. Surgical exposures in revision total knee arthroplasty. Clin Orthop Rel Res 2006;446:59–68.
[6] Burki H, von Knoch M, Heiss C, Drobny T, Munzinger U. Lateral approach with osteotomy of the tibial tubercle in primary total knee arthroplasty. Clin Orthop Rel Res 1999;362:156–61.
[7] Berg EE. Extensile exposure of comminuted patella fractures using a tibial tubercle osteotomy: results of a new technique. J Orthop Trauma 1998;12:351–5.
[8] Maruyama M. Tibial tubercle osteotomy in revision total knee arthroplasty. Arch Orthop Trauma Surg 1997;116:400–3.
[9] Whiteside LA. Exposure in difficult total knee arthroplasty using tibial tubercle osteotomy. Clin Orthop Rel Res 1995;321:32–5.
[10] Wolff AM, Hungerford DS, Krackow KA, Jacobs MA. Osteotomy of the tibial tubercle during total knee replacement. A report of twenty-six cases. J Bone Joint Surg Am 1989;71:848–52.
[11] Eid AS, Nassar WA, Fayyad TA. Total knee replacement with tibial tubercle osteotomy in rheumatoid patients with stiff knee. Int Orthop 2016;40:2289–2293.
[12] Hanschen M, Biberthaler P. Risk factors for failure of osteosynthesis. After periprosthetic fractures of the knee joint. Orthopade 2014;43:541–8.
[13] Mendes MW, Caldwell P, Jiranek WA. The results of tibial tubercle osteotomy for revision total knee arthroplasty. J Arthroplast 2004;19:167–74.
[14] Whiteside LA, Ohl MD. Tibial tubercle osteotomy for exposure of the difficult total knee arthroplasty. Clin Orthop Rel Res 1990;260:6–9.
[15] Whiteside LA. Exposure options in the difficult knee. Orthopedics 2001;24:895–6.
[16] Dolin MG. Osteotomy of the tibial tubercle during total knee replacement. A report of twenty-six cases. J Bone Joint Surg Am 1990;72:790.
[17] Davis K, Caldwell P, Wayne J, Jiranek WA. Mechanical comparison of fixation techniques for the tibial tubercle osteotomy. Clin Orthop Rel Res 2000;380:241–9.
[18] Caldwell PE, Bohlen BA, Owen JR, Brown MH, Harris B, Wayne JS, et al. Dynamic confirmation of fixation techniques of the tibial tubercle osteotomy. Clin Orthop Rel Res 2004;424:173–9.
[19] Werner BC, Evans CL, Carothers JT, Browne JA. Primary total knee arthroplasty in super-obese patients: dramatically higher postoperative complication rates even compared to revision surgery. J Arthroplast 2015;30:849–53.
[20] Jonas SC, Shah R, Mitra A, Deo SD. 5-year cost/benefit analysis of revision of failed unicompartmental knee replacements (UKRs); not "just" a primary total knee replacement (TKR). The Knee 2014;21:840–2.
[21] Piedade SR, Pinaroli A, Servien E, Neyret P. Tibial tubercle osteotomy in primary total knee arthroplasty: a safe procedure or not? The Knee 2008;15:439–46.
[22] Chen YN, Lee PY, Chang CW, Ho YH, Peng YT, Chang CH, et al. Biomechanical investigation of titanium elastic nail prebending for treating diaphyseal long bone fractures. Australas Phys Eng Sci Med 2016;40:115–26.
[23] Chen YN, Lee PY, Chang CH, Chang CW, Ho YH, Li CT, et al. Computational comparison of tibial diaphyseal fractures fixed with various degrees of prebending of titanium elastic nails and with and without end caps. Injury 2016;47:2339–46.
[24] Chang CW, Chen YN, Li CT, Peng YT, Chang CH. Role of the compression screw in the dynamic hip-screw system: a finite-element study. Med Eng Phys 2015;37:1174–9.
[25] Regmi P, Cox AG, Robison CI, Karcher DM. Correlation analysis of cortical geometry of tibia and humerus of white leghorns using clinical quantitative computed tomography and microcomputed tomography scans1. Poult Sci 2017;96(8):2950–5.
[26] Snyder SM, Schneider E. Estimation of mechanical properties of cortical bone by computed tomography. J Orthop Res Off Publ Orthop Res Soc 1991;9:422–31.
[27] Morgan EF, Keaveny TM. Dependence of yield strain of human trabecular bone on anatomic site. J Biomech 2001;34:569–77.
[28] Boresi AP, Schmidt RJ, Sidebottom OM. Advanced mechanics of materials. New York: John Wiley & Sons, Inc.; 1993.
[29] Adams JD Jr, Tanner SL, Jeray KJ. Far cortical locking screws in distal femur fractures. Orthopedics 2015;38:e153–6.
[30] Bottlang M, Lesser M, Koerber J, Doornink J, von Rechenberg B, Augat P, et al. Far cortical locking can improve healing of fractures stabilized with locking plates. J Bone Joint Surg Am 2010;92:1652–60.